IEEE Access
Multidisciplinary ⋮ Rapid Review ⋮ Open Access Journal

Received January 4, 2021, accepted January 7, 2021, date of publication January 11, 2021, date of current version January 15, 2021.

Digital Object Identifier 10.1109/ACCESS.2021.3050934

A Bayesian Optimization Approach for Water Resources Monitoring Through an Autonomous Surface Vehicle: The Ypacarai Lake Case Study

FEDERICO PERALTA SAMANIEGO[1], DANIEL GUTIÉRREZ REINA[1], SERGIO L. TORAL MARÍN[1], MARIO ARZAMENDIA[2], AND DERLIS O. GREGOR[2]

[1]Department of Electronic Engineering, Technical School of Engineering of Seville, 41004 Seville, Spain
[2]Faculty of Engineering, National University of Asuncion, San Lorenzo 111421, Paraguay

Corresponding author: Federico Peralta Samaniego(fperalta@us.es)

This work was supported in part by the Universidad de Sevilla through the Contract "Contratos de acceso al Sistema Español de Ciencia, Tecnología e Innovación para el desarrollo del programa propio de I + D + i de la Universidad de Sevilla", in part by the Spanish "Ministerio de Ciencia, Innovación y Universidades, Programa Estatal de I + D + i Orientada a los Retos de la Sociedad" through the Project "Despliegue Adaptativo de Vehículos no Tripulados para Gestión Ambiental en Escenarios Dinámicos" under Grant RTI2018-098964-B-I00, in part by the regional government Junta de Andalucía through the Project Despliegue Inteligente de una red de Vehículos Acuáticos no Tripulados para la monitorización de Recursos Hídricos under Grant US-1257508, and in part by the regional government Junta de Andalucía through the Project Despliegue y Control de una Red Inteligente de Vehículos Autónomos Acuáticos para la Monitorización de Recursos Hídricos Andaluces under Grant PY18-RE0009.

ABSTRACT Bayesian Optimization is a sequential method for obtaining the maximum of an unknown function that has gained much popularity in recent years. Bayesian Optimization is commonly used to monitor the surface of large-scale aquatic environments using an Autonomous Surface Vehicle. We propose to model water quality parameters using Gaussian Processes, and propose three different adaptations of classical Acquisition Functions in order to explore an unknown space, considering surface vehicle restrictions. The proposed Sequential Bayesian Optimization system uses the aforementioned information in order to monitor the Lake and also to obtain a water quality model, which has an associated uncertainty map. For evaluation, the Mean Squared Error of the resulting approximated models are compared. Afterwards, they are compared with other monitoring algorithms, like the Traveling Salesman Problem, using Genetic Algorithms and Lawnmower. Concluding remarks indicate that the proposed method not only performs better while minimizing the Mean Squared Error (via active monitoring), but also manages to quickly identify an approximate of the black-box function, which is very useful for monitoring lakes like Ypacarai Lake ($60 km^2$) in Paraguay. Additionally, the proposed method reduces the MSE by 25% when compared with Traveling Salesman Problem-based monitoring algorithms and also provides a more robust solution, i.e., 30% more independent of initial conditions, when compared with known robust coverage methods like the lawnmower method.

INDEX TERMS Bayesian optimization, Bayes methods, Gaussian processes, data acquisition, environmental monitoring, informative path planning, autonomous vehicles.

I. INTRODUCTION

Lakes around the world serve as water reservoirs, touristic points, fishing spots and even wildlife beds, among other usages, so their health is of the upmost importance. Maintaining their waters as fresh and as healthy as possible must be a desired and common practice of every human being. Nevertheless, in the absence of this practice, water contamination will rise, and therefore, water resources will not be able to provide the same status as before. The current state of Ypacarai Lake (Paraguay) is an example of this situation (Fig. 1). The lake is having periodical blooming of cyanobacteria [1], caused by eutrophication.[1]

The first step towards eradicating this toxic alga is creating monitoring systems that are capable of providing a spatial

The associate editor coordinating the review of this manuscript and approving it for publication was Yanbo Chen.

[1]As defined in [2], eutrophication is the enrichment of water by nutrients, especially nitrogen and phosphorus, which produces an undesirable alteration to water quality and causes an accelerated growth of algae.

FIGURE 1. Example of the blue-green algae situation found on the shores of Ypacarai Lake, Paraguay. This alga is gives off a fetid odor and toxic to humans and animals.

FIGURE 2. Example of an Autonomous Surface Vehicle for lake monitoring. Catamarans are usually the selected due to their enhanced stability.

distribution map of water quality parameters, such as pH, turbidity, CO2 levels, Dissolved Oxygen, etc. The water quality models (usually presented as a spatial distribution map or contour graph) will help to locate the main contamination spots as well as any unnatural behavior of the water. Therefore, monitoring is one of the most important steps to manage the contamination situation. Autonomous Surface Vehicles (ASVs) (Fig. 2) that are able to reach positions within a lake and perform measurements of water quality are considered suitable for the task [3].

The environmental monitoring techniques that use ASVs are usually designed to explore every zone of the search space. These methods are costly for large scale environments and they generally do not provide water quality models that can be updated or used for future purposes. In real life scenarios, the cost of performing measurements is high due to the indirect costs of reaching the destination point. Consequently, most constraints are related to energy consumption and reaching defined positions. With an infinite horizon of time, an accurate model can be obtained with a confidence of 100%; however, this solution is certainly costly and inefficient. Although monitoring a defined space and obtaining a mathematical model of the same space are considered different missions, both tasks can be accomplished at the same time because of the nature of Bayesian Optimization (BO). Thus, in this work, BO is used as a Mission Planning System in order to obtain both measurements locations and a model of the water quality parameters.

BO, which is based on Bayesian inference, has two main components: i) a surrogate model and ii) an acquisition function or utility function. The Bayesian process begins when the surrogate model is first used as a prior model, and given a set of observations, the Bayes rule is used to obtain a posterior model that fits the given data. The surrogate model predicts how the real scenario (water resource) behaves. Gaussian Processes (GPs) are normally employed as surrogate models since they can determine the uncertainty of the predictions [4], and previous experience can be incorporated in the definition of the kernel. In this work, the surrogate model will supersede a real water quality parameter model; therefore, the nature of the used kernels should be based on the variability of such water quality parameters. Regarding the acquisition, it is used to calculate a maximum over the current model so as to achieve maximum information benefit in the next sample. In the target monitoring task, this maximum value is used to determine the next water quality measurements performed by the ASV. Notice that the acquisition function is very important in the proposed monitoring work because it defines the movements of the ASV. Thus, classical acquisition functions used in BO cannot be directly applied to the monitoring problem due to the mobility restrictions of an ASV. In this work, we proposed several adaptations of the classical acquisition functions that are more suitable for monitoring tasks.

The proposed BO-based Mission Planning system presents important advantages over the exploration or patrolling techniques. First, the ASV will be monitoring and at the same time obtaining a model of the water quality [5]. Second, it can significantly reduce the time required to obtain a model or contamination map, with a given desired confidence level, of a large water resource through an efficient and intelligent sampling mechanism. This fact is important since ASVs are normally supplied by batteries. However, the suitable BO planning of an ASV for monitoring task requires to analysis and adaptation of the main components of BO. As such, in this work we study and compare the main kernels used in BO (Constant, RBF, Matérn, etc.). Their respective hyperparameters have been selected according to the predicted behavior of a simulated ground truth based on the Ypacarai lake. With respect to the acquisition functions,

some novel adaptations are presented and evaluated that can be added on top the classical methods (Probabilistic Improvement, Expected Improvement, etc.), such as: i) masking the acquisition function according to the position of the vehicle, ii) truncating the path segment between the position of the vehicle and the optimal position, defining a new location in the direction of the optimal value, and iii) splitting the path segment from the starting position to the optimal into smaller segments to ensure that the vehicle performs a certain number of measurements before travelling a certain total distance.

The main contributions of this work are:

- The application of Bayesian Optimization for sequential decision making in a water quality monitoring scenario using an ASV.
- The hyperparametrization and comparison of classical kernel functions as surrogate models for water quality distribution maps.
- The proposal of three adaptations of acquisition functions based on classical techniques for monitoring missions using an ASV.
- The comparison of the proposed approach with other exploration algorithms such as Lawnmower and Genetic Algorithm.

This paper continues as follows: Section II presents the related work, focusing on monitoring works. Section III states the problem, the assumptions and the road map to real life applications, Section IV defines the BO framework and describes the proposed approach. Next, Section V describes the setup and execution of the simulations and the results of the proposed method, as well as a comparison with other coverage approaches. Finally, Section VI contains the conclusions of this work.

II. RELATED WORK

This section contains current research efforts corresponding to monitoring systems using ASVs. Although the state of the art includes numerous works, to the best of the authors knowledge, this work is one of the first to carry out monitoring of large bodies of water using BO-based mission planning systems for ASVs.

Conventional methods of monitoring include lawnmower or sweeping algorithms, which consist of exploring the space using a predefined distance between measurement locations and a pre-established route morphology. In general, when using these techniques monitoring occurs slowly. Therefore, these are the preferred methods whenever neither time-related restrictions nor expensive exploration costs are present. L-Cover, T-Cover and Z-cover [6] are some common methods and they fall into the lawnmower category. These methods are extremely useful in situations where the work or search space is very narrow, such as with rivers and streams; however, they have lesser impact observational-wise as the water body widens due to energy availability concerns. In addition, these methods do not provide online learning. Various coverage, patrolling and monitoring works can be found that use unmanned vehicles to accomplish the task of monitoring. Some of them [7], [8] develop control systems for ASVs and are tested in real life scenarios.

Although using multiple vehicles to accomplish coverage escapes the scope of this work, the idea is very useful because it facilitates information gathering at the cost of having a multi robot system coordinator, or a decentralized framework. In [9], multiple Dubins vehicles (capable of following only soft curved paths, i.e., no hard turns or rotation about their axes) were used to perform coverage in a 200 km^2 lake. The vehicles can be heterogeneous as well, implying different physics, dynamics and control for each agent. For example, in [10], the authors developed a coordinated system using an Autonomous Underwater Vehicle (AUV) with an ASV to detect pollution in water environments. Another study [11] proposes a multi-robot path planning algorithm whenever connectivity constraints are present.

A comprehensive survey on robot path planning [12] classifies these works into strategies and approaches that fulfill the coverage mission. The cited applications range from mapping and surveillance to coastal coverage. It is important to highlight that monitoring tasks are not exclusively for surface vehicles, since multiple works use Autonomous Aerial Vehicles (AAVs) to perform the same mission. In [13], the authors present an algorithm that monitors an environment using an energy-constrained AAV that covers an area together with an Autonomous Ground Vehicle (AGV). The work in [14] shows that AAVs can be used to inspect rice farms using Particle Swarm Optimization (PSO) algorithms.

Informative Path Planning (IPP) algorithms can be used for surveying underwater algae farms [5], using Gaussian processes as surrogate models and information gain-based functions to select viewpoints. Another IPP implementation [15] uses AAVs to map unknown environments via ray-casting for mazes and buildings explorations using a Rapidly-Exploring Random Tree star (RRT*) inspired algorithm. Another example that uses ASVs for environmental monitoring can be found in [16], where orienteering-based approaches are proposed.

Some works have focused on developing monitoring systems for Ypacarai Lake [3]. For example, the International Hydroinformation Center (CIH) [17] of Itaipú focuses on continuously monitoring fixed locations within the Lake as well as its main sources of inflow and outflow. Also, the Multidisciplinary Technology Research Center (CEMIT) provides the results of sampling measurements performed in 14 different locations. In [3], the authors propose algorithms that explore the lake with an ASV using Travelling Salesman Problem (TSP)-based evolutionary algorithms, which provides a global path that manages to explore the surface of the Ypacarai Lake. In the TSP algorithm, a set of locations within a working space are defined that must be visited exactly once. Furthermore, in [18], the TSP-based work is expanded and Eulerian circuits are used to solve the path planning problem, instead of Hamiltonian circuits (TSP based path planning). In [19], an efficient strategy for

monitoring algae blooms using TSP algorithms was presented. More recently, in [20], the authors trained a neural network using Deep Reinforcement Learning based on the Markov Decision Process (MDP) for the patrolling problem of the Ypacarai Lake.

Regarding BO-based approaches, recent monitoring proposals using AAV include [21]–[23]. In [21], the authors use Sequential BO in order to obtain a height map using an AAV, where the decision is made using a Partially-Observable Markov Decision Process (POMDP). The obtained results indicate that the Bayesian approach is useful whenever the number of measurements is limited. In [22], continuous 3D trajectories are generated to map an area using Gaussian Processes. Similarly, a path planning model is proposed in [23], where an interactive multiple model algorithm is used to update the belief space. Large scale pollution and luminosity monitoring simulations were performed in [24] using continuous BO approaches, obtaining a significant error reduction compared to other methods. A Bayesian Exploration-Exploitation approach for online planning was presented in [25], using a POMDP utility function. A recent work [26] shows the development of save navigation procedures for mobile robots using BO to predict high movement vibrations in a defined space.

A summary of the works described in this section is presented in Table 1, where the objective is to compare different deployments of autonomous vehicles that are aimed at obtaining information about their environment. The works are ordered by year of publication (2009-2020). Pre-established Routes (PR) are monitoring algorithms whose goal positions are defined by a human operator. These works are control-oriented but manage to monitor areas according to their objectives.

Although the previous works are promising, the proposed method presents some important advantages with respect to the application of real monitoring task applications. The main benefits include: i) obtaining a mathematical surrogate model of a real water quality parameter model, which can be easily used for future purposes, ii) intelligent determination of measuring locations using adapted acquisition functions that take into account the mobility restrictions of autonomous vehicles, and iii) an important reduction of the exploration cost of a water resource, which is crucial for an efficient large-scale monitoring.

TABLE 1. Brief summary of monitoring systems using autonomous vehicles.

Ref.	Objective	Monitoring Algorithm	Vehicle
[25]	Localization and Mapping	PODMP - BO	ground
[24]	Large-Scale Pollution Monitoring	Continuous Trajectory generation using BO	aerial
[24]	Luminosity Monitoring	Continuous Trajectory generation using BO	ground
[10]	Underwater Water Sampling	Lawnmower and Loiter	underwater and aquatic
[21]	Obtaining elevation maps	POMDP - BO	aerial
[14]	Rice Farms inspection	Pre-established Route (PR)	aerial
[7]	Discrete Measuring and Water Sampling	PR	aquatic
[8]	Water Sampling	PR	aquatic
[6]	Bathymetric survey	L-cover and T-cover (Lawnmower related)	aquatic
[16]	Level Set Estimation	Skeleton based Orienteering IPP	aquatic
[19]	Algae bloom monitoring	TSP with Genetic Algorithms	aquatic
[13]	Rows of Crops Coverage	TSP-based with recharging mechanism	aerial and ground
[5]	Underwater algae surveying	BO-based IPP using a camera	underwater
[15]	Building exploration and reconstruction	RRT*-inspired Exploring algorithm	aerial
[22]	Discrete/Continuous variable mapping	Covariance Matrix Adaptation Evolution Strategy	aerial
[20]	Environmental patrolling/monitoring	MDP solved w/ Deep Reinforcement Learning (DDQL)	aquatic

III. STATEMENT OF THE PROBLEM

The objective of the monitoring system is to obtain water quality models accurately and efficiently for the Ypacarai lake. The monitoring system contains an ASV that measures water quality. For the purpose of this work, the Total Distance Travelled (TDT) by the ASV is assumed to be proportionate to the invested energy required to conduct the movement. Therefore, the ASV should travel as little as possible, performing the least possible n number of measurements in order to obtain water quality models with a good confidence level.

In the context of water monitoring, the real water quality model is mathematically defined as the target or objective function $f(\mathbf{x})$, where the input $\mathbf{x}$ corresponds to an (x, y) location in the lake. The ASV is responsible for performing n measurements in an environment in a sub-space of the $\mathbb{R}^n$ space. For this purpose, the vehicle is equipped with a water quality sensor S, which can take samples and store their values in a vector $\mathbf{s} = \{s_i \mid i = 1, 2, \ldots, n\}$, where i corresponds to the measurement number. The ASV associates the ith read with a location p_i where the measurement has been performed. The locations are stored in a vector $\mathbf{p} = \{p_i \mid i = 1, 2, \ldots, n\}$. The data provided by the ASV is denoted by $D = \{(p_i, s_i) \mid i = 1, 2, \ldots, N\}$, assigning the

vehicle's position p_i as the input vector x_i, and a sensor read s_i as the output value, so that, for each D_i,:

$$s_i = f(p_i) \tag{1}$$

This expression can be used to find the regression that estimates the relationship between the water quality values y and the locations $\mathbf{x}$ in the entire domain of the Ypacarai Lake.

$$y \approx f(\mathbf{x}) \tag{2}$$

With sufficient data D, the real function $f(\mathbf{x})$ can be approximated.

For evaluating the surrogate models, there are some usual metrics such as Absolute Error, Mean Squared Error (MSE), or even the robust estimators shown in [27], [28]. The MSE is normally used in regression problems; therefore, it is a suitable performance metric to evaluate the obtained model. The MSE is calculated using (3), where $f(\mathbf{x})$ is the ground truth or real contamination map and y the resulting prediction of the surrogate model. In this case, the ground truth represents the distribution map of the water quality in the Ypacarai lake.

$$\text{MSE}(f(\mathbf{x}), y) = \frac{1}{n_{\text{samples}}} \sum_{i=0}^{n_{\text{samples}}-1} (f(\mathbf{x}_i) - y_i)^2 \tag{3}$$

It is important to indicate that the total travelled distance plays a more important role than the number of measurements performed, even though they are correlated. The reason is that the distance travelled is related to power required by the ASV and it is well-known that energy is one the main limitations of autonomous systems. Therefore, the monitoring system should be as efficient as possible in terms power consumption.

A. ASSUMPTIONS AND CONSIDERATIONS

Several assumptions are considered in the proposed monitoring system based on an ASV.

- **Ypacarai Lake:** The monitoring space is modelled as a $m \times n$ matrix $\mathcal{M}$, where each element $\mathcal{M}_{i,j}$ has a value defined by an occupancy state (1 if the element corresponds to an occupied $d \times d$ square space in the space, 0 if not). The matrix $\mathcal{M}$ can be seen as an image of dimensions $m \times n$, where each pixel is a square of side d, painted white if any kind of obstacle (land, prohibited zones, natural obstacles, etc.) is found within or black otherwise. Fig. 3 shows the model of Ypacarai Lake used in this work, which has been previously used in [29]. It is a non-convex set, consequently, a local path planner is needed to ensure that the vehicle can travel from one point to another.
- **Guidance, Navigation & Control (GNC):** Fig. 4 presents the proposed block diagram of the GNC system of the ASV. The ASV is capable of travelling between locations on the surface of the lake and performing measurements only when it is still. The GNC is fully capable of performing the task of travelling, using a positioning system that has a resolution $\approx d$. Therefore, the ASV is located with a good but not perfect resolution. The GPS error is also simulated, shifting the goal position by a few meters (<25), so that the ASV does not perform measurements in the optimal locations. For simulations purposes, direct movement between the ASV's current position and its goal is allowed as long as the segment crosses no obstacles, otherwise a local path planner is used, which provides routes that avoid obstacles found in the path (see Fig. 4). The RRT* algorithm is selected as local path planner due to its small path planning calculation time [30]. Both the Navigation system and the Control system (low-level) will be executed by an autopilot software/hardware embedded system, such as the Navio2[2] or Pixhawk4.[3]
- **Water quality measurements:** Despite being capable of performing multiple measurements of different quality parameters (Dissolved Oxygen, power of Hydrogen, Total Dissolved Solids, etc.), only the MSE of one water quality variable is minimized at a time. Moreover, the values of measurements have standard attributes ($\mu(\mathbf{x}) = 0$, $\sigma(\mathbf{x}) = 1$) and noise is negligible. As real values of water quality parameters are not defined with a mean of zero, an additional function to normalize the parameters is required. In addition, we consider that water quality parameters are stationary during the monitoring task.
- **Vehicle autonomy:** Battery usage and time consumption are considered through the maximum distance that the ASV can travel. Performance tests performed using the ASV shown in Fig. 2 shows that it can travel at a maximum velocity of 2 m/s for 2.1 hours, it can cover approximately 15000 linear meters. Therefore, this distance is the baseline that for comparison in this work.

FIGURE 3. Occupancy grid model of the Ypacarai Lake. It is a non-convex set because there exist segments made with two black positions which crosses white zones.

IV. PROPOSED APPROACH

The monitoring approach proposed in this paper is based on BO. The main objective consists of minimizing the uncertainty of an unknown water quality model. BO is defined

[2]https://navio2.emlid.com/
[3]https://pixhawk.org/

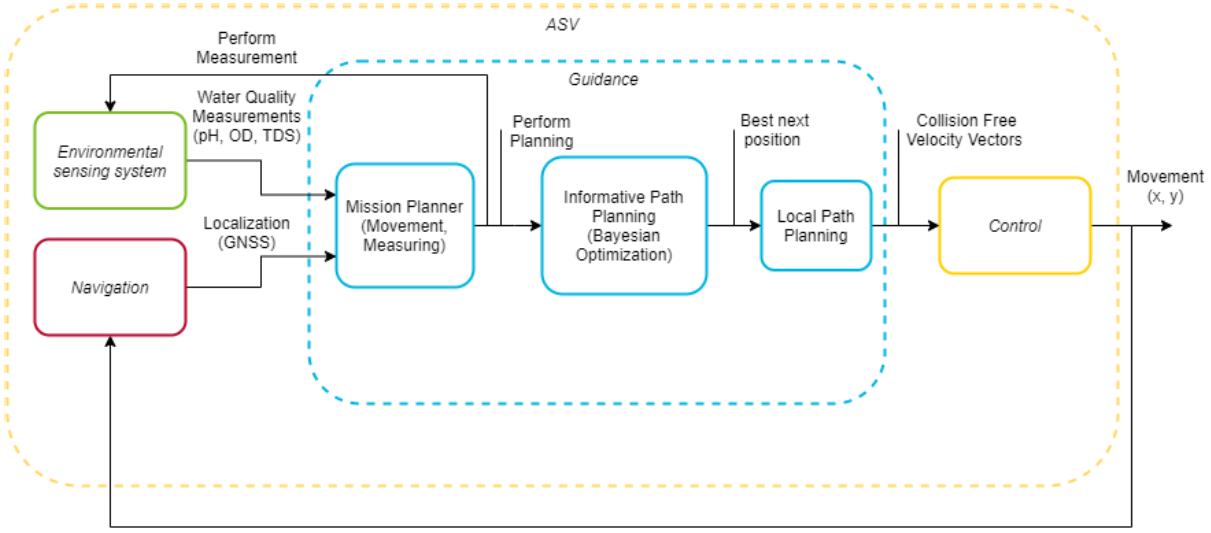

FIGURE 4. Proposed general ASV diagram. It includes the main GNC system and also an Environmental Sensing system, which provides discrete water quality information.

by three components: the surrogate model, the acquisition or utility function and an optimization algorithm. In the proposed approach, these components are tailored for the monitoring task of an ASV.

A. BAYESIAN OPTIMIZATION FOR MONITORING

BO is a sequential strategy used for obtaining the global optimal point (global maximum or minimum) of a function that has expensive evaluation costs [31]. For the monitoring task, the application of this method is not straightforward, since in this context obtaining the maximum/minimum value of a function is not the main objective. Nevertheless, with the appropriate selection of the main components of BO, such as the kernel and the acquisition function, we will demonstrate that BO is a suitable tool that is able to provide confident models with a small number of samples.

The general steps of BO are shown in Fig. 5. For surrogate modelling, BO uses Bayes theorem Eq. (4) to infer a posterior belief of a black box function given by a likelihood function and a prior belief [4]

$$P(f|D) = P(D|f) \times P(f) \tag{4}$$

The expression indicates that the informed surrogate model $(f|D)$ is proportionate to the data collected by the sensors $(D|f)$ and the prior (f). The prior incorporates the belief about the shape or smoothness of the target function. In water monitoring context, it includes the knowledge about the quality model to be obtained. The likelihood term reflects the data that the ASV is sampling and the posterior is the updated model once the new samples are incorporated. After the posterior model is fitted through a Gaussian Regression Process (GPR), it can predict the values for the search space. Then, an AF is used over the predictions of the posterior model to determine the optimal location for a new data sample D_{i+1}. Therefore, the optimization of the AF determines the next movement of the ASV. The monitoring ends whenever a specified level of certainty of the model is reached.

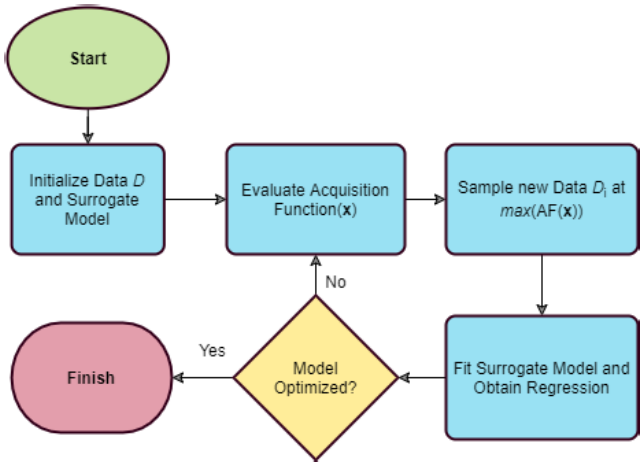

FIGURE 5. Sequential Bayesian Optimization procedure. The initializing procedure can include a fitting if there is any prior information. The decision block will return an affirmative value if a condition of collected information is met.

Next, we describe the GPR used to fit the model, the classical AFs used in BO and the proposed modifications tailored for monitoring task of an ASV.

B. GAUSSIAN PROCESS REGRESSIONS (GPR)

Gaussian Processes (GPs) are generally used as a surrogate model in the Bayesian inference for both the prior and posterior model. Since they are based on multivariate Gaussian distributions, they can fit data with ease (some examples include [5], [21], [26]). GPs are defined with a mean function $\mu(\mathbf{x})$ and a covariance function. or kernel $k(x, x')$, defined as

$$\begin{aligned} \mu(\mathbf{x}) &= \mathbb{E}[f(\mathbf{x})] \\ k(\mathbf{x}, \mathbf{x}') &= \mathbb{E}[(f(\mathbf{x}) - \mu(\mathbf{x}))(f(\mathbf{x}') - \mu(\mathbf{x}'))] \end{aligned} \tag{5}$$

The target function can be approximated to the GP as follows

$$f(\mathbf{x}) \sim GP(\mu(\mathbf{x}), k(\mathbf{x}, \mathbf{x}')) \tag{6}$$

For any kernel and some measured data $\mathcal{D}$, it can be demonstrated [4] that, after fitting, the GP can predict the mean values and standard deviation of the target function, giving a posterior using (7). The posterior consists in a Normal or Gaussian Distribution $\mathcal{N}(0, \sigma)$.

$$\begin{bmatrix} y_1 \\ y_2 \\ \vdots \\ y_n \end{bmatrix} \sim GP(\mu(\mathbf{x}), k(\mathbf{x}, \mathbf{x}')) = \mathcal{N}(0, \sigma) \tag{7}$$

Covariance functions, or *kernels*, are the functions that provide a measure of similarity between two random input variables and thus are a crucial component of GP. There are plenty of ways to describe relationships between variables, but as the desired regressor should be able to describe a 2-D map of a supposedly continuous spread of a quality measure (water quality parameters in lake environments are expected vary smoothly across the surface), the studied kernels should provide correlations that will produce models that are as smooth as possible.

Kernels are modelled as a matrix K, such as the element $K_{i,j} = k(\mathbf{x}_i, \mathbf{x}_j)$ represents the covariance between two inputs. This matrix should always be positive semidefinite, implying that relations between all inputs can be found, forming a square matrix. In order to obtain the posterior distribution, the kernel matrix is augmented to include covariances between the test inputs (not measured locations that need to be inferred) $\mathbf{x}*$ with themselves and the covariances with the known data $\mathbf{x}$ using

$$K = \begin{bmatrix} K & K_* \\ K_*^T & K_{**} \end{bmatrix} = \begin{bmatrix} k(\mathbf{x}, \mathbf{x}) & k(\mathbf{x}, \mathbf{x}*) \\ k(\mathbf{x}*, \mathbf{x}) & k(\mathbf{x}*, \mathbf{x}*) \end{bmatrix} \tag{8}$$

Finally, the surrogate model can predict the mean $\mu_{y_*|D}$ and uncertainty $\sigma_{y_*|D}$ of unknown data using the next expressions:

$$\mu_{y_*|D} = K_*^T (K + \epsilon^2 I)^{-1} y \tag{9}$$

$$\sigma_{y_*|D} = K_{**} - K_*^T (K + \epsilon^2 I)^{-1} K_* \tag{10}$$

K_* describes the covariance between the collected data D and the unknown data, and K_{**} refers to the covariance of the unknown data. Both are sub-matrices of the kernel K that can be easily be obtained by applying the covariance function to the input of data D augmented with the input to predict. In [4], the authors include a noise function ϵ that is used if there is a need to consider noisy data input. This noise can be modelled after Gaussian, Laplacian or uniform functions [32] but in the scopes of this work, noises are negligible. GPs can provide water quality models of entire spaces with high accuracy if sufficient data is supplied. Furthermore, accurate posterior models can be obtained if appropriate covariance functions are selected.

TABLE 2. Kernels in gaussian processes.

Kernel f.	Expression	Hyperp.
Constant	${\sigma_0}^2$	σ_0
RBF	$\exp\left(-\frac{r^2}{2\ell^2}\right)$	ℓ
RQ	$\left(1 + \frac{r^2}{2\alpha\ell^2}\right)^{-\alpha}$	ℓ, α
Matérn	$(2^{\nu-1}\Gamma(\nu))^{-1}(\frac{r\sqrt{2\nu}}{\ell})^{\nu} K_\nu(\frac{r\sqrt{2\nu}}{\ell})$	ℓ, ν

1) COVARIANCE FUNCTIONS

The most commonly-used covariance functions are presented in Table 2, showing the expressions and their respective hyperparameters. In Table 2, r corresponds to Euclidean distance between two vector inputs $\mathbf{x}, \mathbf{x}'$.

For the target monitoring task through an ASV, a suitable kernel should be selected. To this aim, we assume that water quality functions are stationary in terms of the input, i.e., the lake has homogeneous properties so that the same behavior can be found anywhere in the lake. Therefore, stationary kernels are selected and studied.

As follows, we describe the most used stationary kernels in GPs:

- **Constant kernel:** A standard covariance function denoted by ${\sigma_0}^2$, which determines the average distance of a target value away from the mean of the function. Usually, ${\sigma_0}^2$ is present in most of the kernels.
- **Squared Exponential (SE):** The most widely-used kernel in this field, also known as RBF (Radial Basis Function). It is a function that captures the covariance within a range of [0, 1]. This kernel has a hyperparameter ℓ that corresponds to a length scale that describes the smoothness of the function. It provides a measure of how far two different inputs can be in order to affect or influence each other. The higher the value of ℓ, the slower the rate of change. Moreover, larger values provide more extrapolation limits.
- **Rational Quadratic (RQ):** A kernel that represents an infinite sum of RBFs with different characteristic length scales. As the infinite sum can be correlated to a scale mixture, the RQ kernel expects that the objective function will behave smoothly across many length scales. The hyperparameters are ℓ, which behaves exactly like RBF, and α, that corresponds to the scale mixture parameter. As α tends to ∞ RQ approximates to a regular RBF.
- **Matérn class:** A kernel capable of fitting less homogeneous data. It has two positive hyperparameters: ν and ℓ. The first defines the smoothness of the function (i.e., the greater the value the smoother, up to $\nu \to \infty$ where the Matérn function becomes the SE.) while the latter defines the length scale of the kernel. This covariance function also incorporates two functions $\Gamma(\nu)$ and K_ν which correspond to the Gamma Function and Modified Bessel Function of second order, respectively. In several works [4], [33], ℓ is usually defined as an integer and ν as a half-integer: $\ell + 1/2$.

C. GENERAL ACQUISITION FUNCTIONS

AF are used to determine the projected utility of measuring one specific point within the environment. Then, the maximum of the AF represents the best possible next point to measure or sample.

The process for obtaining a new measurement position in this work differs from common approaches as the assumptions of the search space are also different. Water bodies environments are generally non-convex sets and the definition of the space is also limited to where the water or the terrain are present. This constraint leads to the acknowledgement that the monitoring space is not continuous on the shores of the lake, as no water quality information can be obtained in the terrain. With these assumptions, commonly-used fast optimizers like the limited-memory Broyden-Fletcher-Goldfarb-Shanno algorithm (L-BFGS) or the Newton-Conjugate Gradient (N-CG) cannot be used as they only behave correctly whenever the search space is continuous. In our case, we proceed to calculate the AF value for every point in the map that is associated with a water zone. Therefore, the optimization process corresponds to fully observing the search space (using an AF) and picking the maximum/minimum position within the lake.

There are several widely-used functions that balance exploration/exploitation [33]. Usually in BO-based sequential decision-making, an agent seeks to explore near the beginning of the mission and exploit the maximum/minimum values at the end. Therefore, most AFs are designed to accomplish this task and for this reason they include an explicit exploration/exploitation parameter ξ, which helps balancing the AF evaluation. Classical AFs are explained below:

- **Probability of Improvement (PI):** It computes the probability of obtaining a value that is better than a the current maximum. It relies on the Cumulative Distribution Function (CDF) $\Phi(Z)$ of the normalized surrogate model Z. According to [33], Z depends on the current minimum measured value $f(\mathbf{x}^+)$ and has the form of

$$Z = \frac{f(\mathbf{x}^+) - \mu(\mathbf{x}) - \xi}{\sigma(\mathbf{x})} \tag{11}$$

  The probability of improvement of a location can be obtained using

$$PI(\mathbf{x}) = \Phi(Z) \tag{12}$$

- **Expected Improvement (EI):** It improves the PI function using the predictive uncertainty to prevent the exploitation bias that occurs when only the probability of improving is considered. Therefore, EI uses not only the CDF but also the Probabilistic Density Function (PDF). EI returns a measure of optimization beliefs based on the current CDF $\Phi(\mathbf{x})$ and PDF $\phi(\mathbf{x})$ of the standardized normal Z. The exploration/exploitation balance is implicitly found in this AF. The predictive mean (found in the first term of 13) manages the exploitation weights, while the predictive uncertainty $\sigma(\mathbf{x})$ provides more exploration weight as it increases. The following corresponds to the EI expression

$$\mathrm{EI}(\mathbf{x}) = \begin{cases} 0 & \text{if } \sigma(\mathbf{x}) = 0 \\ (f(\mathbf{x}^+) - \mu(\mathbf{x}) - \xi)\Phi(Z) & \\ +\,\phi(Z)\sigma(\mathbf{x}) & \textit{else} \end{cases} \tag{13}$$

- **Scaled Expected Improvement (SEI):** It is an extension of EI method that has been proposed in [34]. In this function the $\mathrm{EI}(\mathbf{x})$ is scaled to favor selecting points where the improvement has a small variance, but the predicted value is expected to be high. The scaling factor $\mathbb{V}[I(\mathbf{x})]$ is computed as

$$\mathbb{V}[I(\mathbf{x})]^2 = k(\mathbf{x}, \mathbf{x})[(Z^2 + 1)\Phi(Z) + Z\phi(Z)] - \mathrm{EI}(\mathbf{x})^2 \tag{14}$$

  The SEI is expressed as

$$\mathrm{SEI}(\mathbf{x}) = \frac{\mathrm{EI}(\mathbf{x})}{\mathbb{V}[I(\mathbf{x})]} \tag{15}$$

- **Max-value Entropy Search (MVES):** It is a function that quantifies the information gain about the supposed maximum of a function $f(\mathbf{x})$ [35]. It values the negative differential entropy of the posterior maximum input using the next expression

$$\mathrm{MVES}(\mathbf{x}) \approx \frac{Z\Phi(Z)}{2\phi(Z)} - \log(\phi(\mathbf{x})) \tag{16}$$

Classical AFs provide useful results in BO when they are employed to optimize costly functions. However, they present some limitations related to their application to the monitoring task of an ASV. Therefore, additional work is required to adapt them so that BO can be applicable in large-scale water environmental monitoring tasks.

D. PROPOSED ACQUISITION FUNCTIONS

To overcome the limitations of classical AF for the monitoring task of an ASV, this work proposes new adaptations for them to include mechanisms to encourage selecting points that are near the vehicle's current position. Three different adaptations have been designed and tested; each one focuses on reaching optimal measurement locations as well as selecting points not far from the ASV's current position.

Fig. 6(a) shows an example of ground truth that will be used to illustrate the results of the proposed AF. It has three different maximum values and it shows the positions where previous measurements have been taken. Using these measurements, a posterior model GP is calculated and used to determine the output of AFs. Next, Fig. 6(b) shows the output of the SEI AF without any modification. Although this example used SEI, all classical AFs can be used with the proposed adaptations. The blue marker corresponds to the next position where the ASV will perform a measurement, which corresponds to the maximum value of the AF. As follows, we describe the proposed adaptations of AFs, which are shown in the other subfigures in Fig. 6.

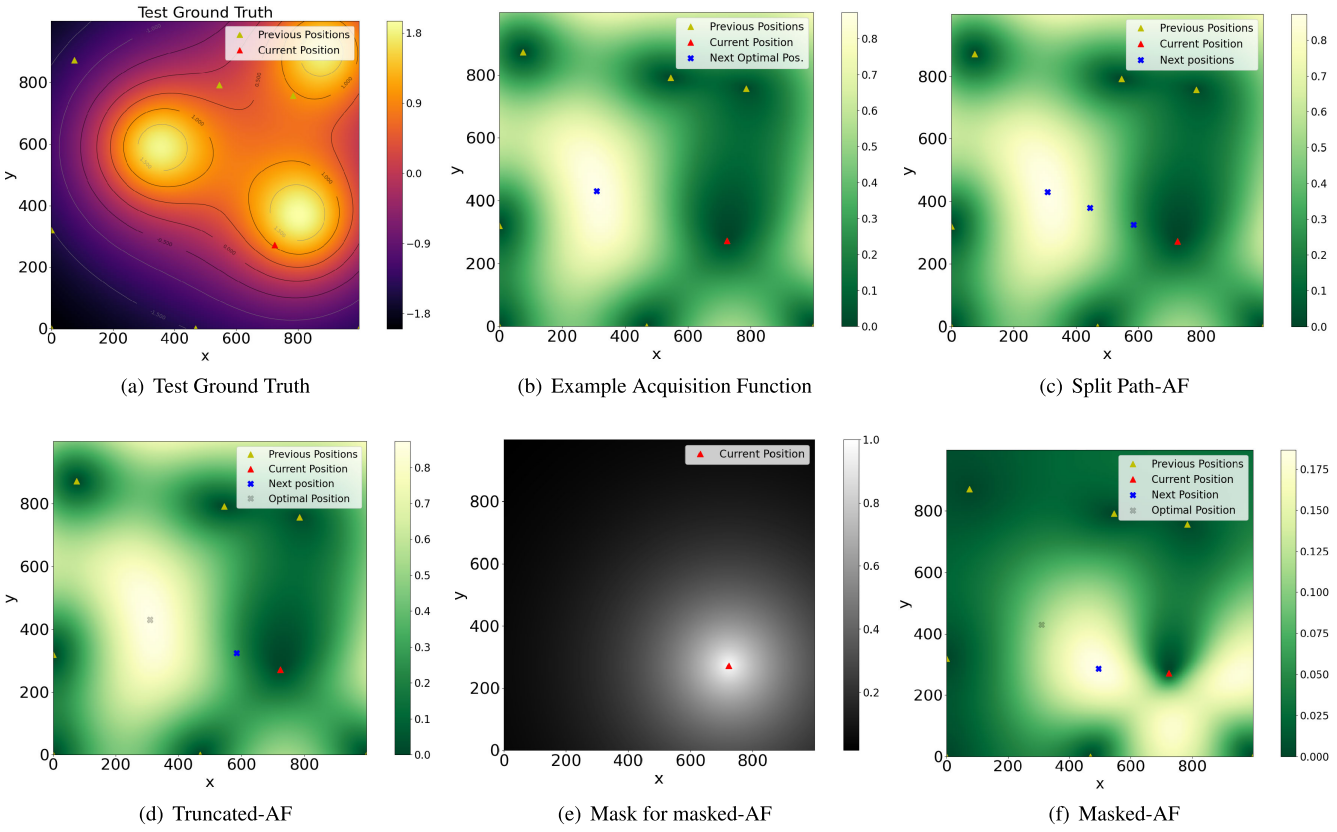

(a) Test Ground Truth (b) Example Acquisition Function (c) Split Path-AF

(d) Truncated-AF (e) Mask for masked-AF (f) Masked-AF

FIGURE 6. **Different adaptations of an example AF (Scaled-EI). The first sub-image corresponds to the ground truth, where 3 maxima are defined. The red triangle represents the current position of the vehicle, yellow triangles: position of previous measurements. The next sub-images (except for (c)) present the values of the AF. The locations where the ASV should perform the evaluations are marked with a blue cross. The optimal value is marked with a black cross, if the optimal is not equal to the proposed next location. The sub-figure (c) provides an insight of the mask that the ASV will use to define the next location, according to the masked-adaptation.**

- **Split Path:** The main idea is to leverage the long distances travelled from one sample position to another in classical AFs. During long distances the ASV can take several samples before updating the surrogate model. This method calculates the new target location according to classical AFs and the current ASV position. Then, a set of measurements are taken within the segment from the vehicle's position and the target point. These locations are equally distanced between each one of them by a constant l, which defines the average distance that the ASV should travel in order to perform a new measurement. Fig. 6(c) shows the waypoints defined by using the AF with the split path adaptation. The vehicle should visit all goals (the three blue markers) and perform measurements on each point, but only will fit the surrogate model and calculate next optimal position whenever measurements on all points have been performed. The travelled distance between waypoints will generally be equal l, except on the last path or whenever the locations are zones with known obstacles.
- **Truncated Path:** In this method the direct path to the next target location according to the AF is truncated after a distance l. The idea is to take into account the mobility restrictions of ASV so it should not travel long distances before updating the surrogate model. Notice that the next optimal sampling in location is the same used in split path method (depicted in gray color Fig. 6(d)) since it is defined by the underlying AF. However, in this case the distance travelled by the ASV is truncated, reaching a suboptimal location (depicted in blue color in Fig. 6(d)). It can be observed that the blue position is aligned with the current-optimal positions segment. Whenever the ASV reaches this position and updates the data, a new goal location is obtained using the selected AF. This new location is generally not the same as split path-adaptation because of the new information provided.
- **Masked Path:** This method weights the nearby locations using a simple gradient according to (17), where x corresponds to the locations on the search space and p the position of the ASV. An example mask is shown in Fig. 6(e), which is used to mask the result found by the classical AFs, producing the masked-AF (Fig. 6(f)). This process is done by multiplying the mask with the result of the unmodified AF, as shown in (17). This method allows exploiting the current position of the ASV in

TABLE 3. Summary of properties of the proposed adaptations.

Adaptation	Distance b/w new data locations and ASV	Measurements before GP Fitting step
Split path-	$l, 2l, \ldots, nl, d$	$n+1$
Truncated-	l	1
Masked-	generally $<= l$	1

order to obtain more information with less movement.

$$\mathbf{M} = \exp \frac{-(||\mathbf{x} - p||)}{l} \tag{17}$$

A summary of the proposed adaptations is included in Table 3, showing that they only depend on a tunable hyperparameter l. It is important to highlight that each one has a distinctive characteristic with respect to updating the surrogate model. The split path-adaptation will perform at least one or more measurements before fitting the Gaussian model. The two others will strictly fit the model after each measurement. The truncated-adaptation provides the information to the ASV in its path to the maximum, so it can quickly update the model. Finally, masked-adaptation favors the maximum of nearby locations.

V. PERFORMANCE EVALUATION

In this section, the proposed method based on BO is evaluated for monitoring a simulated aquatic environment. First, we define a general ground truth model based on Ypacarai Lake, then simulation results are presented in different test groups. The first group compares different kernels for monitoring the Ypacarai Lake. Next, with a selected kernel, classical AFs are tested. Then, the best AFs are modified with our proposed adaptations and evaluated in the case study scenario. Finally, the best configuration (kernel, adapted-AF) is compared with other monitoring algorithms.

A. SIMULATION SETUP

This section defines the procedures and parameters for the evaluation of the proposed method. The code for this section is available online[4] and has been developed for python 3.8.4. The simulations have been conducted in a laptop computer with 32GB RAM, Intel i7 3.2 GHz processor.

1) GROUND TRUTH OR SIMULATED WATER QUALITY MODEL FOR YPACARAI LAKE

Water quality models often follow a smooth function due to fluid dynamics and wind conditions [1], [2]. In that sense, test scenarios for validating the proposed method can be modelled as smooth functions, such as Bohachevsky or Himmelblau. However, their gradients have big values, which are not usual for environmental parameters. In contrast, the Shekel Multimodal Function (SMF) can be adjusted to provide maximum zones with gentle gradients. Additionally, the SMF can have

[4]https://github.com/FedePeralta/BO_drones

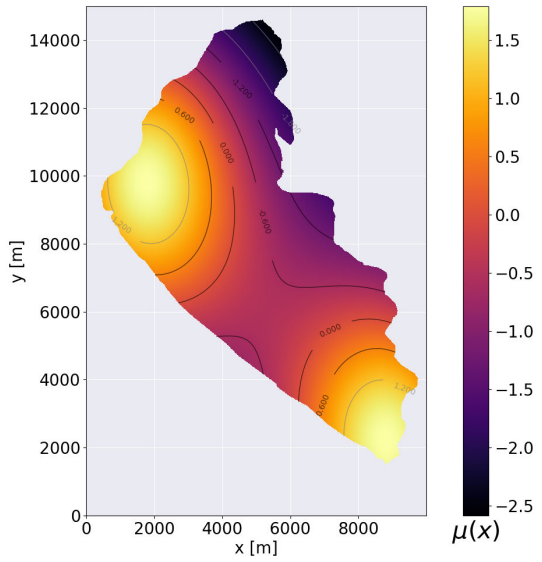

FIGURE 7. Ground Truth for a simulated water quality parameter using a Shekel-based function, scaled. The model has $\mu(\mathbf{x}) = 0$, $\sigma(\mathbf{x}) = 1$.

any number of maximum values, which fairly simplifies the setup procedure for obtaining the ground truth for each simulation run. SMF has the form of:

$$f_{\text{Shekel}}(\mathbf{x}) = \sum_{i=1}^{M} \frac{1}{c_i + \sum_{j=1}^{N} (\mathbf{x}_j - a_{ij})^2} \tag{18}$$

where c_i and a_{ij} correspond to the elements of two given set of matrices A and c with sizes MxN and $Nx1$, respectively. M is the desired number of maximum values and N the number of dimensions. The simulation area is modelled as $\mathcal{M}$ with dimensions 1000×1500, where each element $\mathcal{M}_{i,j}$ corresponds to a square with side $d \sim 10[m]$.

The map shown in Fig. 7 is an example of a test configuration, where there are two defined maximum values in the lake. The parameter values of each position x, y are taken from the result of a standardized shekel function scaled up. The domain of the shekel function is defined in the range $[0, 1]$ for each dimension, and the shekel input matrices are defined as $A = [[0.16, 0.67], [0.9, 0.13]]$ and $c = [0.15, 0.15]$. The locations of the maximum values have been selected according to the two main towns in contact with the Ypacarai lake [1] (Areguá and San Bernardino). Both of them are touristic points, which would imply deviations from the mean of a water quality parameter. For instance, an inappropriate disposal of waste could increase the turbidity of the water. Fig. 7 shows two peaks in the mentioned zones, which represent a high value of turbidity (turbidity sensor), a distinctive green color (RGB color sensor), high pH variance (pH sensor), or any other quality parameter with values higher than usual.

While the original values of the function range from 3.65 to 7.70, the values for the ground truth range approximately from -2.6 to 1.8, which helps the GP fit data more easily. For real life applications, where the ground truth is unknown,

TABLE 4. Mean of n simulations Mean Squared Errors with their respective 95% confidence interval for different GP kernels. MSE $= \mu \pm 1.96\sigma$.

Kernel	Hyperparameters	MSE ($n = 15$)
RBF	$\ell = 100$	0.0707 ± 0.2111
Matérn	$\ell = 100$, $\nu = 3.5$	0.08 ± 0.2236
Rational Quadratic	$\ell = 100$, $\alpha = 0.1$	$\mathbf{0.0705 \pm 0.2111}$

by applying the Central Limit Theorem (CLT), the measured data can be modified by dividing the difference between the real value and the expected mean by the expected (or maximum allowed) variance.

Initial Data D corresponds to the normalized values provided by two stations (Club Náutico San Bernardino (CNSB) and Playa Municipal Areguá (PMA)) of the CIH [17]. The initial position of the ASV is selected randomly. Therefore, with p_0 as the initial position of the ASV $D = (p_{CNSB}, s_{CNSB}), (p_{PMA}, s_{PMA}), (p_0, s_0)$, the initial data to fit the GP is composed of three samples.

2) PERFORMANCE METRICS

As stated in Section III, MSE is the selected metric used for evaluating the performance of the proposed method. For the kernel and classical AF selection, the distance between points is not relevant since they are not dependent on the environment constraints. Therefore, the MSE is compared with the number n of samples performed by the ASV. For the proposed AFs, the main evaluation is performed whenever the ASV travelled a total of 15000 m.

B. KERNEL SELECTION

The covariance functions to be tested (RBF, RQ, Matérn) are all dependent on the hyperparameter ℓ. For the expected quiet waters of Ypacarai lake [1], the length scale should be sufficiently large to ensure smoothness, but bounded to provide the kernel enough freedom to adapt to varying maximum/minimum data. We propose that $\ell \sim 10\%$ of the length of the search space. For other hyperparameters, if any, the most common values [4], [33] are used.

Fifty different simulations have been conducted for the kernel selection, each test using both different seeds and differing sets of 15 uniformly drawn points. The results included in Table 4 show that for the Ypacarai Lake, RBF and RQ have the best MSE. Consequently, either of these kernels could be indifferently selected. As RQ is the generalization of RBF, it is expected that RQ is a more complex expression in terms of computational requirements. For this reason, RBF is the selected kernel for the proposed BO-based monitoring system and it will be used as the prior/posterior model for the next simulations.

C. ACQUISITION FUNCTION SELECTION

This subsection has the objective of evaluating the classical AFs for the simulated Ypacarai Lake. The idea is to select the best classical AF that will serve as underlying method for the proposed modifications. Once the best classical AF is selected, the proposed modifications have been implemented on top of it to compare their performances. The ASV has the initial data D mentioned in V-A1 and it has the capabilities and restrictions mentioned in this work. New samples are taken once the ASV travels from its current position to the optimal value per AF. In order to ensure a fair comparison among AFs, the simulations have been performed with the same random seeds. After a new measurement is conducted, the total distance travelled in meters is saved along with the MSE and the number of measurements. For the comparison framework, the mean and standard deviation of the MSE and the Total Distance Travelled (TDT) of each method is obtained.

TABLE 5. Acquisition function behavior test. The value *n* corresponds to the number of measurements performed.

Acquisition f.	Hyperparameters	MSE ($n = 15$)
Probability of Improvement	$\xi = 0.01$	0.2960 ± 0.1988
	$\xi = 1.0$	$\mathbf{0.0170 \pm 0.0163}$
Expected Improvement	$\xi = 0.01$	0.0421 ± 0.0498
	$\xi = 1.0$	0.0193 ± 0.0204
Scaled EI	$\xi = 0.01$	0.0380 ± 0.0362
	$\xi = 1.0$	0.0189 ± 0.0167
Max-value Entropy Search	$\xi = 0.01$	0.5366 ± 0.1864
	$\xi = 1.0$	0.6382 ± 0.3704

1) CLASSICAL ACQUISITION FUNCTIONS

For each one of the classical AFs presented in this work, two sets of simulations have been run, one with $\xi = 0.01$ and the second using $\xi = 1.0$. Notice that as ξ factor increases, the AF increases its exploration behaviors over exploitation. Due to the fact that classical AFs are not distance dependent, the comparison is made between the number of measurements performed instead of the TDT. The results are shown in Table 5. It can be observed that the PI with $\xi = 1.0$ has the lowest MSE with a 95% confidence interval. Notice that the figures present non-negligible confidence intervals; this is to be expected as the ASVs do not start on the same position for each one of the 50 simulations, which affects the behavior of the monitoring system and thus the MSE. Fig. 8 shows a bar graph where the MSE of each method (using the best ξ) is displayed for each measurement. Notice that each bar shows the 95% confidence interval. Also, Fig. 8 shows that PI, EI and SEI with $\xi = 1.0$ behave similarly after 15 steps. Therefore, only the MVES AF should be discarded while the other classical AFs should be considered for the proposed adaptations and evaluations.

2) PROPOSED ACQUISITION FUNCTIONS

The next step is to apply the proposed adaptations to the selected AFs in order to add the mobility restrictions of

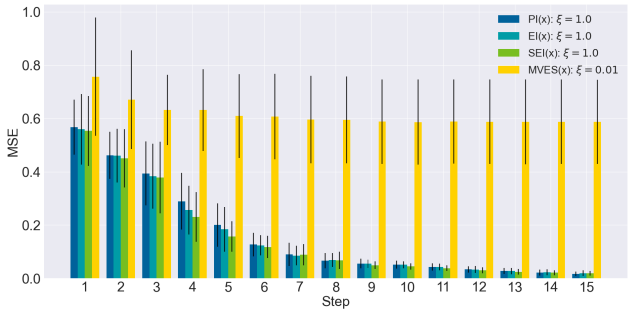

FIGURE 8. MSE using different acquisition functions. The best set of simulations for each AF is used. The confidence intervals are approximately equal for the first three AFs (PI, EI and SEI).

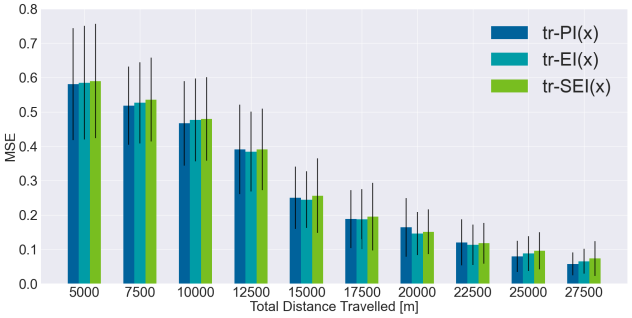

FIGURE 9. MSE using the truncated-adaptation on the same acquisition functions (PI, EI, SEI).

TABLE 6. Proposed acquisition functions behavior test.

Adaptation	Acquisition Function	MSE ($TDT = 15000m$)	Average Calc. Time [s]
Split path-	$PI(\mathbf{x})$	0.2897 ± 0.2130	1.8581
	$EI(\mathbf{x})$	0.2913 ± 0.2147	2.1947
	$SEI(\mathbf{x})$	0.3129 ± 0.2569	1.7015
Truncated-	$PI(\mathbf{x})$	0.2498 ± 0.1773	1.7222
	$EI(\mathbf{x})$	$\mathbf{0.2445 \pm 0.1614}$	1.8356
	$SEI(\mathbf{x})$	0.2561 ± 0.2133	1.8870
Masked-	$PI(\mathbf{x})$	0.4171 ± 0.2791	1.9878
	$EI(\mathbf{x})$	0.4179 ± 0.2773	1.8102
	$SEI(\mathbf{x})$	0.3520 ± 0.2176	1.7694

the ASV. In these simulations, the number of simulations is the same as in the previous evaluation, but the number of measurements performed has been increased by 5. Table 6 shows the results after the ASV has travelled a distance of 15000 m. It can be seen that the best proposed adaptation is the truncated method, which provides both the lowest MSE mean and confidence interval. Additionally, Table 6 shows the average calculation time to solve the GPs and obtain a measurement location using an adapted-AF. The MSE for this method is shown in Fig. 9. It can be observed that the three methods are set to converge after ∼30000 m and they provide approximately the same mean for MSE. Furthermore, the tr-$EI(\mathbf{x})$ generally provides the lower confidence interval, obtaining more robust results. Analytically, EI AF is also less biased towards exploitation, which is a good property in monitoring situations.

For visualization, an example of the generated water quality models for the best run using the proposed method is shown in Fig. 10. For each column, the upper row corresponds to the surrogate model GP mean and the lower to the standard deviation, or uncertainty, of the GP. It can be observed that whenever new measurements (red triangles) are performed, the resulting GP mean is more alike the ground truth (Fig. 7). Consequently, the monitoring system based on the ASV is working well. It is important to indicate that the following seven MSE (plus two initial samples) is only 0.07, and the standard deviation is always <0.6 in the whole search space. Therefore, the achieved results by the proposed method are remarkable.

D. COMPARISON WITH OTHER MONITORING APPROACHES

Having selected the best overall combination (kernel and AF with proposed modifications), the next objective is to compare the proposed method with other monitoring techniques found in the literature. The best path planning provided by a Genetic Algorithm (GA) proposed in [19] and a Lawnmower (LM) algorithm as found in [36] are both applied to Ypacarai Lake are candidates for comparison. In order to use the same metric (MSE) for comparison, some changes have been applied to both the GA and LM approaches. Assuming that measurements cannot be performed continuously and that both methods define long segments for monitoring, the techniques should divide their segments into smaller ones that are similar in size to the median distance between measurements of the best result in Table 6. Another change made to the GA and LM methods is that GPs are used to infer the water quality model provided using both GA and LM measurement data so that the MSE can be calculated to be compared later. In each case, the overall mean distance between measurements performed using the truncated-$EI(\mathbf{x})$ technique has been used to define the minimum distance that GA and LM should travel before performing a new measurement. With this distance set, both methods are used in simulations, obtaining measurements are updating their GPR.

For the sake of a fair comparison, this subsection is divided into two parts. First, we compare the proposed methods with respect to the defined ground truth of the water quality parameters. Second, we generalize the comparison by comparing the methods over a number of random ground truths.

1) DEFINED GROUND TRUTH

The results are shown in Table 7 (MSE after 15000 m) as well as in Fig. 11.It can be seen that the proposed method clearly outperforms the others. Also, Fig. 11 shows that the proposed method improves over time. The standard deviation of the BO after 50 simulations is also the best, implying that generally the proposed method provides better results.

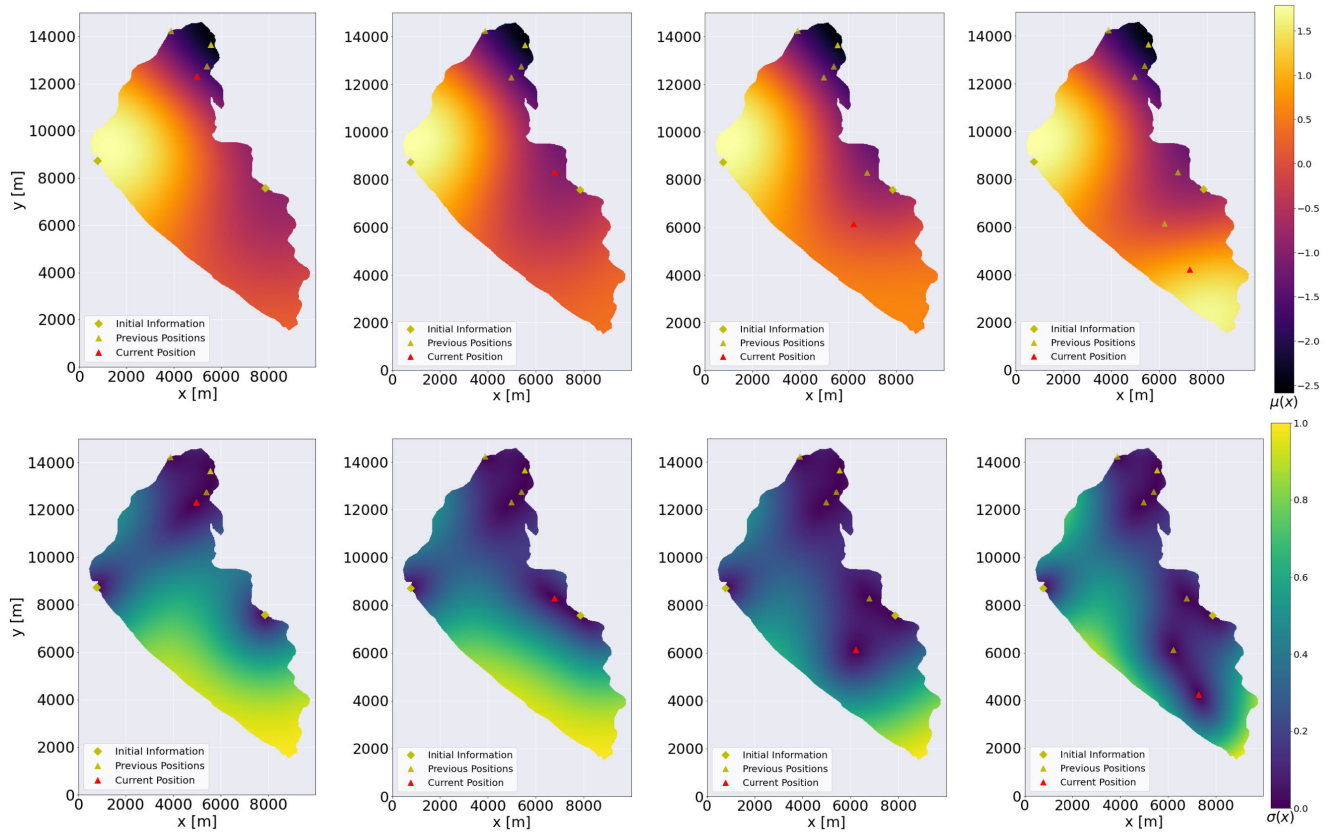

(a) $n = 4$ (b) $n = 5$ (c) $n = 6$ (d) $n = 7$

FIGURE 10. Example of Sequential Bayesian Optimization for lake monitoring. The system manages to perform the monitoring as well as obtaining a water quality model at the same time.

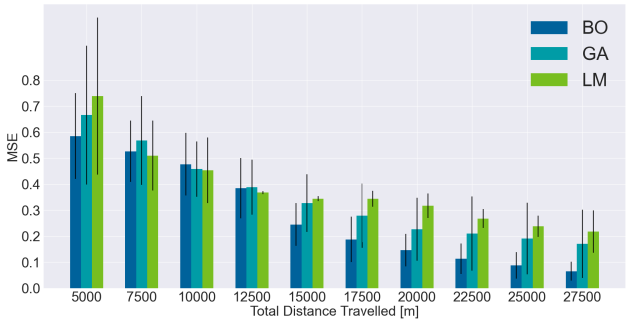

FIGURE 11. Mean Squared Error vs. Total Distance Travelled comparison for our proposed method (BO), the monitoring path planning using Genetic Algorithms (GA) and the Lawnmower (LM) method.

Fig. 12 shows a comparison of the evaluated methods after 15000 m. For each column, the mean of the GP and the squared error with the ground truth is shown. It can be observed that, while GA and LM methods manage to carefully learn certain zones, they fail to provide a good overall response with the same distance travelled. The proposed BO-based method selects points that represent accurately a subsection of the search space. Furthermore, after travelling an approximate total of 15000 m, the number of measurements performed by the BO and the LM method is 10, while the GA performed 11.

TABLE 7. Comparison of the proposed method with Genetic Algorithms and Lawnmower applied to monitoring Ypacarai Lake.

Method	MSE ($TDT = 15000m$)
Proposed Method	$\mathbf{0.2445 \pm 0.1614}$
Genetic Algorithm	0.3273 ± 0.2173
Lawnmower	0.3442 ± 0.0189

2) GENERALIZATION WITH RANDOM GROUND TRUTHS

For generalization, 10 random ground truths are used to compare the approaches using the SF. We define $m \in [2, 6]$ random maximum locations with approximately the same factor c within the work space. In total, 500 simulations for both BO and GA (50 simulations for each ground truth) and 40 for LM (4 simulations each ground truth) were performed. The results are shown in Fig. 13. While the difference in the confidence interval of the methods is not as big as the difference using the selected ground truth, the resulting MSE is always better using the proposed method.

E. COMPUTATIONAL EFFICIENCY

As GP are non-parametric regressions, the more data is acquired, the more computationally inefficient the regression

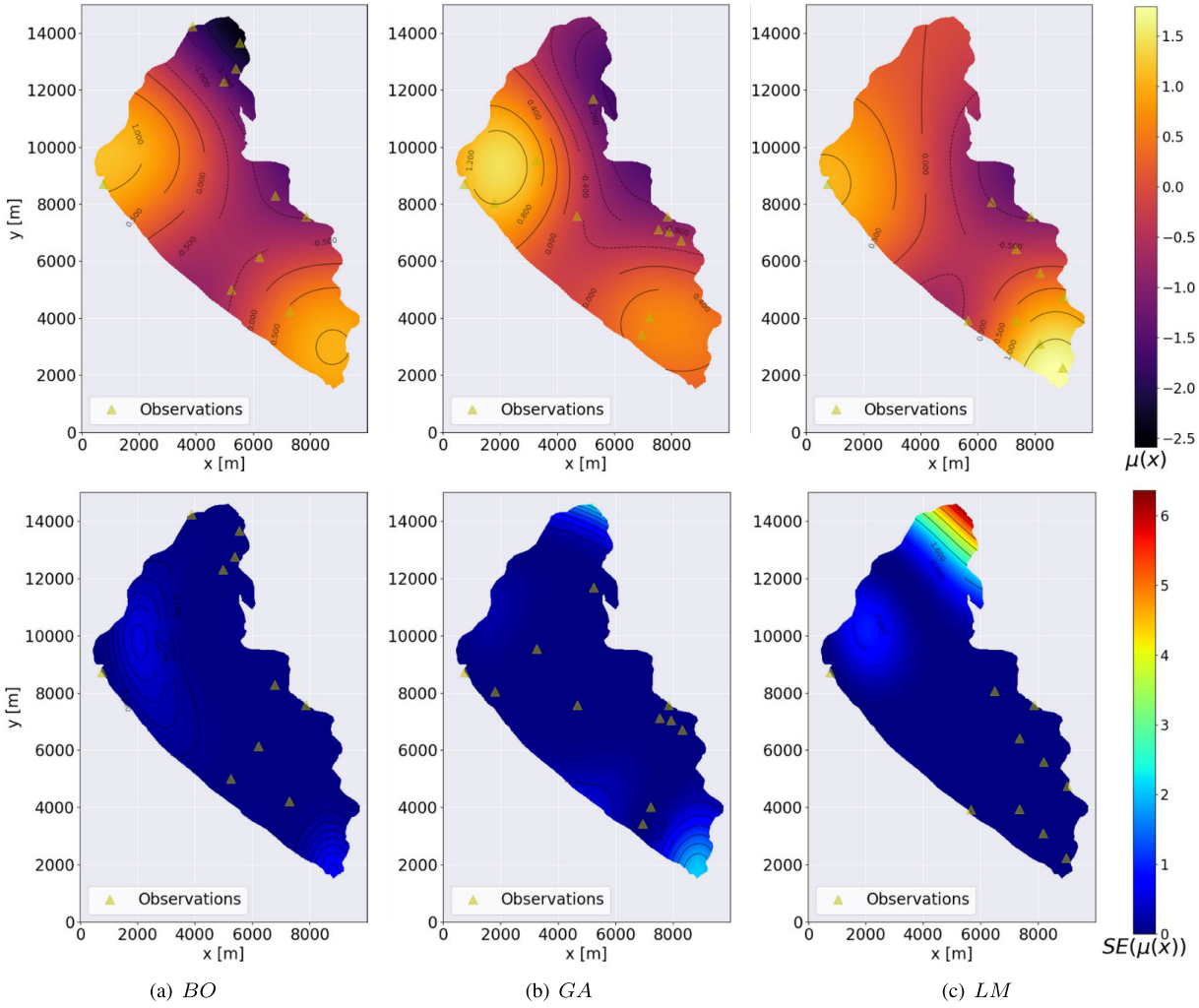

FIGURE 12. Comparison of the mean of GP (upper row) and Squared Error (lower row) for the BO, GA and LM methods, respectively.

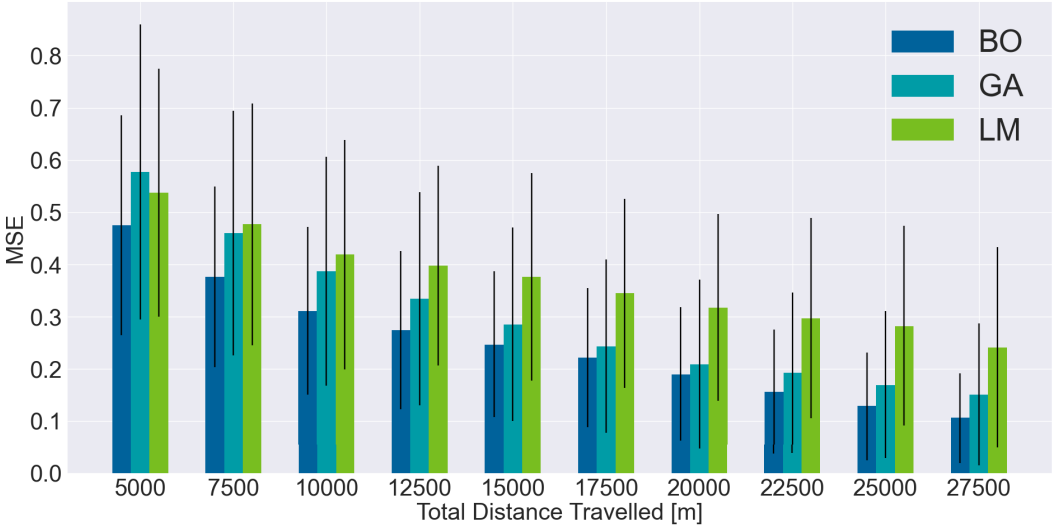

FIGURE 13. Resulting MSE vs TDT using 10 different random ground truth (50 simulations each ground truth).

becomes. The three methods compared in this work use GPs to provide inferences, but only our method is dependent on it. This is due to the fact that our proposed method intelligently provides new waypoints for every iteration on any situation using AFs, which makes the method an online or active learning algorithm. On the other hand, GA and LM methods both provide PR (Pre-established Routes), and while the GA method used in these comparisons is considered an intelligent monitoring algorithm that can update the waypoints offline, the LM method cannot update to provide new locations and is not an intelligent monitoring algorithm. These considerations make the computational efficiency non comparable.

Since our method relies on solving GPs (and subsequently using an AF) after each measurement, it can be assumed that BO cannot be applied during real life scenarios. However, as seen in Table 6, our method is proven to be optimal in time-related constraints. As the value shown is the median, it is necessary to state that the BO method takes a shorter amount of time to provide a result at the early stages of the monitoring but takes increasingly more time after new measurements are added to data D. Naturally, this represents that there is a limit of measurements that can be performed before the method becomes infeasible for real-time calculations of new locations. To overcome this particular situation, in [37], the authors present a review on scalability of GPs and current techniques for big data fitting such as Sparse Kernels or Sparse Approximations. In any case, our proposed method is suitable for the water monitoring objective and is easily scalable using the aforementioned techniques.

F. DISCUSSION OF THE RESULTS

As follows, we discuss the main results obtained in this work:

- For the studied ground truth, the best kernel in terms of fitting and time consumption is RBF. The hyperparameter value ℓ is a suitable option whenever no data is known a priori and is effective. The other kernels adapt successfully to the data and can also be considered for selection in more complex environments, but as the behavior of the water quality parameters is expected to be like the Shekel Function-based ground truth, RBF is a suitable kernel for selection.
- The selection of appropriate AFs is not easy in these scenarios, due to their similarities in terms of MSE (except for MVES). However, it has been observed that EI and SEI generally provide new measurement locations near unknown locations, i.e., weighting exploration over exploitation, as desired.
- The three proposed AF adaptations are demonstrated to be useful. However, after the defined total distance travelled, the truncated adaptation performed the best. The other two methods present some drawbacks. For example, split path has the inconvenience of gathering redundant information, while the masked method quickly disregards useful, but distant locations in non-complex scenarios.
- The proposed ASV and BO-based monitoring approach obtains an accurate model more rapidly than other methods. It has been shown that the proposed approach is also robust with respect to the initial position of the ASV. The generalization test shows that our method and GA algorithm performs averages of 6 measurements before travelling a total distance of 15000 m, but the MSE is significantly lower (25%) using the proposed method.
- The proposed approach clearly outperforms other monitoring approaches with high exploration capabilities, such as GA-based and lawnmower algorithm. For example, when using the proposed ground truth, the MSE of our proposed method is 25% and 29% better than the GA and Lawnmower algorithms, respectively. Similar results were found in the generalization test, with difference of 24.5% and 29%, respectively.
- The computational efficiency of our method is proficient for the constraints that are present in a real life ASV experiment and the amount of measurements it can perform.

VI. CONCLUSION AND FUTURE WORK

This work proposes one of the first BO methods for path planning of an ASV, aimed at minimizing the uncertainty of a contamination distribution of an aquatic environment. We not only tested multiple kernels to obtain the one that best fits the data, but also tested and compared several AFs in order to obtain the best combination of kernel and AF to minimize the MSE of a simulated ground truth in the Ypacarai Lake environment. More importantly, we proposed three different adaptations of classical AFs to deal with the mobility restrictions of the ASVs. Our tests show that the proposed truncated adaptation achieves the best results. Furthermore, we compared the proposed monitoring approach with other alternatives found in the literature, such as the GA-based exploration algorithm and the lawnmower method. The obtained results demonstrated the validity of the proposed approach, since it clearly outperforms the other techniques in the simulated scenarios. For future works, noisy data can be tested with the proposed method as GPs can easily take noise into account, providing a more realistic solution. The proposed method can also be improved with a multi-agent system composed of several ASVs. Using a centralized coordination could decrease the total distance travelled by each ASV through multi-objective optimization.

ACKNOWLEDGMENT

This work was proofread by Inko Bovenzi and Jaime Jimenez.

REFERENCES

[1] G. A. M. L. Moreira, L. Hinegk, A. Salvadore, G. Zolezzi, F. Hölker, R. A. S. M. Domecq, M. Bocci, S. Carrer, L. De Nat, J. Escribá, and C. Escribá, "Eutrophication, research and management history of the shallow Ypacaraí lake (paraguay)," *Sustainability*, vol. 10, no. 7, p. 2426, 2018.

[2] T. C. Malone and A. Newton, "The globalization of cultural eutrophication in the coastal ocean: Causes and consequences," *Frontiers Mar. Sci.*, vol. 7, p. 670, Aug. 2020.

[3] M. Arzamendia, D. Gregor, D. G. Reina, and S. Toral, "A path planning approach of an autonomous surface vehicle for water quality monitoring using evolutionary computation," in *Technology for Smart Futures*. Cham, Switzerland: Springer, 2018, pp. 55–73.

[4] C. Williams and C. Rasmussen, *Gaussian Processes for Machine Learning*, vol. 2. Cambridge, MA, USA: MIT Press, 2006.

[5] C. Chauvin-Hameau, "Informative path planning for algae farm surveying," Ph.D. dissertation, School Elect. Eng. Comput. Sci., KTH, Stockholm, Sweden, 2020.

[6] N. Karapetyan, A. Braude, J. Moulton, J. A. Burstein, S. White, J. M. O'Kane, and I. Rekleitis, "Riverine coverage with an autonomous surface vehicle over known environments," in *Proc. IEEE/RSJ Int. Conf. Intell. Robots Syst. (IROS)*, Nov. 2019, pp. 3098–3104.

[7] T. H. Yang, S. H. Hsiung, C. H. Kuo, Y. D. Tsai, K. C. Peng, K. C. Peng, Y. C. Hsieh, Z. J. Shen, J. Feng, and C. Kuo, "Development of unmanned surface vehicle for water quality monitoring and measurement," in *Proc. IEEE Int. Conf. Appl. Syst. Invention (ICASI)*, Apr. 2018, pp. 566–569.

[8] J. Paez, J. L. Villa, J. Cabrera, and E. Yime, "Implementation of an unmanned surface vehicle for environmental monitoring applications," in *Proc. IEEE 2nd Colombian Conf. Robot. Autom. (CCRA)*, Nov. 2018, pp. 1–6.

[9] N. Karapetyan, J. Moulton, J. S. Lewis, A. Quattrini Li, J. M. Okane, and I. Rekleitis, "Multi-robot dubins coverage with autonomous surface vehicles," in *Proc. IEEE Int. Conf. Robot. Autom. (ICRA)*, May 2018, pp. 2373–2379.

[10] A. Vasilijevic, D. Nad, F. Mandic, N. Miskovic, and Z. Vukic, "Coordinated navigation of surface and underwater marine robotic vehicles for ocean sampling and environmental monitoring," *IEEE/ASME Trans. Mechatronics*, vol. 22, no. 3, pp. 1174–1184, Jun. 2017.

[11] A. Dutta, A. Ghosh, and O. P. Kreidl, "Multi-robot informative path planning with continuous connectivity constraints," in *Proc. Int. Conf. Robot. Autom. (ICRA)*, May 2019, pp. 3245–3251.

[12] R. Almadhoun, T. Taha, L. Seneviratne, and Y. Zweiri, "A survey on multi-robot coverage path planning for model reconstruction and mapping," *Social Netw. Appl. Sci.*, vol. 1, no. 8, p. 847, Aug. 2019.

[13] K. Yu, J. M. O'Kane, and P. Tokekar, "Coverage of an environment using energy-constrained unmanned aerial vehicles," in *Proc. Int. Conf. Robot. Autom. (ICRA)*, May 2019, pp. 3259–3265.

[14] E. Camci, D. R. Kripalani, L. Ma, E. Kayacan, and M. A. Khanesar, "An aerial robot for rice farm quality inspection with type-2 fuzzy neural networks tuned by particle swarm optimization-sliding mode control hybrid algorithm," *Swarm Evol. Comput.*, vol. 41, pp. 1–8, Aug. 2018.

[15] L. Schmid, M. Pantic, R. Khanna, L. Ott, R. Siegwart, and J. Nieto, "An efficient sampling-based method for online informative path planning in unknown environments," *IEEE Robot. Autom. Lett.*, vol. 5, no. 2, pp. 1500–1507, Apr. 2020.

[16] L. Bottarelli, M. Bicego, J. Blum, and A. Farinelli, "Orienteering-based informative path planning for environmental monitoring," *Eng. Appl. Artif. Intell.*, vol. 77, pp. 46–58, Jan. 2019.

[17] Itaipú. (2016). *Centro Internacional de Hidroinformática*. Accessed: Oct. 15, 2020. [Online]. Available: https://hidroinformatica.itaipu.gov.py/

[18] M. Arzamendia, I. Espartza, D. G. Reina, S. L. Toral, and D. Gregor, "Comparison of eulerian and Hamiltonian circuits for evolutionary-based path planning of an autonomous surface vehicle for monitoring ypacarai lake," *J. Ambient Intell. Humanized Comput.*, vol. 10, no. 4, pp. 1495–1507, Apr. 2019.

[19] M. Arzamendia, D. Gutierrez, S. Toral, D. Gregor, E. Asimakopoulou, and N. Bessis, "Intelligent online learning strategy for an autonomous surface vehicle in lake environments using evolutionary computation," *IEEE Intell. Transp. Syst. Mag.*, vol. 11, no. 4, pp. 110–125, winter 2019.

[20] S. Y. Luis, D. G. Reina, and S. L. T. Marin, "A deep reinforcement learning approach for the patrolling problem of water resources through autonomous surface vehicles: The ypacarai lake case," *IEEE Access*, vol. 8, pp. 204076–204093, 2020.

[21] P. Morere, R. Marchant, and F. Ramos, "Sequential Bayesian optimization as a POMDP for environment monitoring with UAVs," in *Proc. IEEE Int. Conf. Robot. Autom. (ICRA)*, May 2017, pp. 6381–6388.

[22] M. Popović, T. Vidal-Calleja, G. Hitz, J. Chung, I. Sa, R. Siegwart, and J. Nieto, "An informative path planning framework for UAV-based terrain monitoring," *Auto. Robots*, vol. 44, pp. 889–911, Feb. 2020.

[23] Y. Qiming, Z. Jiandong, and S. Guoqing, "Modeling of UAV path planning based on IMM under POMDP framework," *J. Syst. Eng. Electron.*, vol. 30, no. 03, pp. 545–554, Jun. 2019.

[24] R. Marchant and F. Ramos, "Bayesian optimisation for informative continuous path planning," in *Proc. IEEE Int. Conf. Robot. Autom. (ICRA)*, May 2014, pp. 6136–6143.

[25] R. Martinez-Cantin, N. de Freitas, E. Brochu, J. Castellanos, and A. Doucet, "A Bayesian exploration-exploitation approach for optimal online sensing and planning with a visually guided mobile robot," *Auto. Robots*, vol. 27, no. 2, pp. 93–103, Aug. 2009.

[26] R. Oliveira, L. Ott, V. Guizilini, and F. Ramos, "Bayesian optimisation for safe navigation under localisation uncertainty," in *Robotics Research*. Cham, Switzerland: Springer, 2020, pp. 489–504.

[27] Y. Chen, J. Ma, P. Zhang, F. Liu, and S. Mei, "Robust state estimator based on maximum exponential absolute value," *IEEE Trans. Smart Grid*, vol. 8, no. 4, pp. 1537–1544, Jul. 2017.

[28] Y. Chen, Y. Yao, and Y. Zhang, "A robust state estimation method based on SOCP for integrated electricity-heat system," *IEEE Trans. Smart Grid*, vol. 12, no. 1, pp. 810–820, Jan. 2021.

[29] F. Peralta, M. Arzamendia, D. Gregor, K. Cikel, M. Santacruz, D. G. Reina, and S. Toral, "Development of a simulator for the study of path planning of an autonomous surface vehicle in lake environments," in *Proc. IEEE Chilean Conf. Electr., Electron. Eng., Inf. Commun. Technol. (CHILECON)*, Nov. 2019, pp. 1–6.

[30] F. Peralta, M. Arzamendia, D. Gregor, D. G. Reina, and S. Toral, "A comparison of local path planning techniques of autonomous surface vehicles for monitoring applications: The Ypacarai lake case-study," *Sensors*, vol. 20, no. 5, p. 1488, Mar. 2020.

[31] E. Brochu, V. M. Cora, and N. de Freitas, "A tutorial on Bayesian optimization of expensive cost functions, with application to active user modeling and hierarchical reinforcement learning," 2010, *arXiv:1012.2599*. [Online]. Available: http://arxiv.org/abs/1012.2599

[32] Y. Chen, F. Liu, S. Mei, and J. Ma, "Toward adaptive robust state estimation based on MCC by using the generalized Gaussian density as kernel functions," *Int. J. Electr. Power Energy Syst.*, vol. 71, pp. 297–304, Oct. 2015.

[33] F. Archetti and A. Candelieri, *Bayesian Optimization and Data Science*. Cham, Switzerland: Springer, 2019.

[34] U. Noè and D. Husmeier, "On a new improvement-based acquisition function for Bayesian optimization," 2018, *arXiv:1808.06918*. [Online]. Available: http://arxiv.org/abs/1808.06918

[35] Z. Wang and S. Jegelka, "Max-value entropy search for efficient Bayesian optimization," 2017, *arXiv:1703.01968*. [Online]. Available: http://arxiv.org/abs/1703.01968

[36] A. Sakai, D. Ingram, J. Dinius, K. Chawla, A. Raffin, and A. Paques, "PythonRobotics: A Python code collection of robotics algorithms," 2018, *arXiv:1808.10703*. [Online]. Available: http://arxiv.org/abs/1808.10703

[37] H. Liu, Y.-S. Ong, X. Shen, and J. Cai, "When Gaussian process meets big data: A review of scalable GPs," *IEEE Trans. Neural Netw. Learn. Syst.*, vol. 31, no. 11, pp. 4405–4423, Nov. 2020.

FEDERICO PERALTA SAMANIEGO was born in Asunción, Paraguay. He received the degree in mechatronics engineering from the National University of Asuncion, Paraguay, in 2019. He is currently pursuing the Ph.D. degree in automatics, electronics and telecommunications engineering with the University of Seville. He is also working as a Research Assistant with the University of Seville. He focuses his work on the development of GNC systems for autonomous vehicles and robotics applications.

DANIEL GUTIÉRREZ REINA received the B.E. degree (Hons.) in electronic engineering, the M.S. degree in electronics and telecommunications, and the Ph.D. degree (Hons.) in electronic engineering from the University of Seville, Seville, Spain, in 2009, 2011, and 2015, respectively. He worked as an Assistant Professor with Loyola University from October 2018 to April 2019. He has been a Visitor Researcher with Liverpool John Moores University, U.K., the Free University of Berlin, Germany, the Colorado School of Mines, USA, and Leeds Beckett University, U.K. He is currently working as an Assistant Professor with the Electronic Engineering Department, University of Seville. He has published about 40 articles in JCR journals with impact factor. His current research interests include the application of meta-heuristic algorithms to solve wireless multi-hop network optimization problems, such as MANETs, VANETs, DTNs, and FANETs. He is a part of the editorial board of several journals, such as *International Journal of Distributed Sensor Networks* (SAGE), *Electronics* (MDPI), *Future Internet* (MDPI), *Wireless Communications and Mobile Computing* (Hindawi), organizing numerous SI for these journals.

SERGIO L. TORAL MARÍN was born in Rabat, Morocco, in 1972. He received the M.S. and Ph.D. degrees in electrical and electronic engineering from the University of Seville, Spain, in 1995 and 1999, respectively. He is currently a Full Professor with the Department of Electronic Engineering, US. He is actually an author or coauthor of 95 articles in major international peer-reviewed journals (with JCR impact factor) and of over 100 articles in well-established international conferences and workshops. His research interests include ad hoc networks and their routing protocols, flying ad hoc networks, deployment of unmanned vehicles, and intelligent transportation systems.

MARIO ARZAMENDIA received the B.E. degree in electrical engineering from the University of Brasilia (UnB), Brazil, the M.S. degree from the University of Mie, Japan, and the Ph.D. degree from the University of Seville, Spain. He is currently a Researcher with the Laboratory of Distributed Systems (LSD), Faculty of Engineering, National University of Asuncion (FIUNA), Paraguay. He is also involved with several projects supported by the National Council of Science and Technology from Paraguay (CONACYT). His research interests include autonomous surface vehicles, metaheuristics optimization, and wireless sensor networks.

DERLIS O. GREGOR was born in Asunción, Paraguay, in 1980. He received the degree in computer engineering in Paraguay, in 2007, and the M.Sc. and Ph.D. degrees in electronic, signal processing and communications in Spain, 2009 and 2013, respectively. He is currently a Teacher Research and the Head of the Distributed Systems Laboratory (LSD), Engineering Faculty, National University of Asuncion (FIUNA), Paraguay. His research interests include the application of intelligent transportation systems (ITS), monitoring and management systems related to the environment, autonomous surface vehicles (ASV), and precision agriculture (PA).